




# A critical role for *miR-142* in alveolar epithelial lineage formation in mouse lung development

Amit Shrestha<sup>1,2</sup> · Gianni Carraro<sup>3</sup> · Nicolas Nottet<sup>4,5</sup> · Ana Ivonne Vazquez-Armendariz<sup>2</sup> · Susanne Herold<sup>2</sup> · Julio Cordero<sup>6</sup> · Indrabahadur Singh<sup>6</sup> · Jochen Wilhelm<sup>2</sup> · Guillermo Barreto<sup>6,7</sup> · Rory Morty<sup>8</sup> · Elie El Agha<sup>1,2</sup> · Bernard Mari<sup>4,5</sup> · Chengshui Chen<sup>1</sup> · Jin-San Zhang<sup>1,9</sup> · Cho-Ming Chao<sup>1,2,10</sup> · Saverio Bellusci<sup>1,2</sup> 

Received: 10 January 2019 / Revised: 5 March 2019 / Accepted: 12 March 2019 / Published online: 18 March 2019  
© Springer Nature Switzerland AG 2019

## Abstract

The respiratory epithelium arises from alveolar epithelial progenitors which differentiate into alveolar epithelial type 1 (AT1) and type 2 (AT2) cells. AT2 cells are stem cells in the lung critical for the repair process after injury. Mechanisms regulating AT1 and AT2 cell maturation are poorly defined. We report that the activation of the glucocorticoid pathway in an in vitro alveolar epithelial lineage differentiation assay led to increased AT2 marker *Sftpc* and decreased *miR-142* expression. Using *miR-142* KO mice, we demonstrate an increase in the AT2/AT1 cell number ratio. Overexpression of *miR-142* in alveolar progenitor cells in vivo led to the opposite effect. Examination of the KO lungs at E18.5 revealed enhanced expression of *miR-142* targets *Apc*, *Ep300* and *Kras* associated with increased  $\beta$ -catenin and p-Erk signaling. Silencing of *miR-142* expression in lung explants grown in vitro triggers enhanced *Sftpc* expression as well as increased AT2/AT1 cell number ratio. Pharmacological inhibition of Ep300- $\beta$ -catenin but not Erk in vitro prevented the increase in *Sftpc* expression triggered by loss of *miR-142*. These results suggest that the glucocorticoid-*miR-142*-Ep300- $\beta$ -catenin signaling axis controls pneumocyte maturation.

**Keywords** Alveolar epithelium · microRNA-142 · Lung · EP300 · Beta-catenin

---

Amit Shrestha and Gianni Carraro contributed equally.

---

**Electronic supplementary material** The online version of this article (<https://doi.org/10.1007/s00018-019-03067-8>) contains supplementary material, which is available to authorized users.

---

✉ Cho-Ming Chao  
Cho-Ming.Chao@paediat.med.uni-giessen.de

✉ Saverio Bellusci  
saverio.bellusci@innere.med.uni-giessen.de

<sup>1</sup> Department of Pulmonary and Critical Care Medicine, The First Affiliated Hospital of Wenzhou Medical University, Wenzhou, Zhejiang, China

<sup>2</sup> Cardio-Pulmonary Institute (CPI), Member of the German Center for Lung Research (DZL), Universities of Giessen and Marburg Lung Center (UGMLC), Justus-Liebig-University Giessen, 35392 Giessen, Germany

<sup>3</sup> Department of Medicine, Cedars-Sinai Medical Center, Lung and Regenerative Medicine Institutes, Los Angeles, CA, USA

<sup>4</sup> Centre National de la Recherche Scientifique, CNRS, UMR 7275, Institut de Pharmacologie Moléculaire et Cellulaire (IPMC), Sophia Antipolis, France

<sup>5</sup> Université Côte d'Azur, Nice, France

<sup>6</sup> Lung Cancer Epigenetics, Member of the German Center of Lung Research (Deutsches Zentrum für Lungenforschung, DZL), Max-Planck-Institute for Heart and Lung Research, 61231 Bad Nauheim, Germany

<sup>7</sup> Institute of Fundamental Medicine and Biology, Kazan (Volga Region) Federal University, 420008 Kazan, Russian Federation

<sup>8</sup> Department of Lung Development and Remodeling, Max Planck Institute for Heart and Lung Research, Bad Nauheim, Germany

<sup>9</sup> Institute of Life Sciences, Wenzhou University, Wenzhou, Zhejiang, People's Republic of China

<sup>10</sup> Department of General Pediatrics and Neonatology, University Children's Hospital Gießen, Justus-Liebig-University, Giessen, Germany

## Introduction

The formation of the alveolar epithelial lineage during lung development is coordinated with the process of branching morphogenesis [1]. Lung development starts at E9.5 with the formation of the laryngotracheal groove on the ventral side of the foregut endoderm. As the trachea separates from the underlying esophagus, the primary lung rudiments appear at the most distal part of the trachea. During the pseudoglandular stage (E9.5–E16.5), the lung epithelium undergoes a coordinated process of branching morphogenesis and differentiation [2]. This allows the formation of a tree-like structure comprised of main branches proximally (the future bronchi) as well as buds. Sox9/Id2-positive cells located at the tip of the epithelial buds during the pseudoglandular stage are considered to be multipotent epithelial progenitor cells [3, 4]. Lineage tracing experiments at E11.5 using *Id2*<sup>CreERT2</sup> showed that Id2<sup>+</sup> epithelial cells at the distal tip can give rise to both bronchiolar and alveolar progenitors [3]. Single cell transcriptomic studies of the developing epithelium at E14.5, E16.5 and E18.5 demonstrated the existence of cells expressing both the alveolar epithelial cell type 1 (AT1) marker *Pdpn* and the type 2 (AT2) marker *Sftpc* at E18.5. These cells are called bipotent (BP) progenitor cells [5]. Based on the expression of several AT1 and AT2 markers, it has been suggested that early bipotent progenitors are already present at E16.5 and can give rise progressively to either AT1 or AT2 during the subsequent phases of lung development. AT1 and AT2 cells lining the alveolar sacs are regarded among the most important pulmonary cells allowing the lungs to function properly by mediating gaseous exchange as well as through surfactant production. Supporting BP cells as common progenitors for AT1 and AT2, it was recently reported that alveolar progenitor cells co-expressing *Pdpn* and *Sftpc* at the lung tip are migrating out of the lumen at E16.5–E17.5 and will be destined to become AT2 as they escape the stretching-induced differentiation effect due to the internal pressure. The authors proposed that the cells remaining in the lumen will then differentiate into AT1 cells [6]. It is important to note that the BP model as progenitor for AT1 and AT2 still needs to be validated using lineage tracing approaches. An alternative and non-mutually exclusive model for AT2 formation is that some of the alveolar progenitor cells never transit through a bipotent intermediate but rather give rise to mature AT2 cells through progressive and direct differentiation.

MicroRNAs (miRs) are small regulatory RNA in mammals that account approximately 1% of the genome. They are 22- to 25-nucleotide-long single-stranded RNAs processed from hairpin transcripts, that regulates

post-transcriptional gene regulation in eukaryotes by binding at the 3'-UTR regions of the target mRNA thus leading to mRNA cleavage, degradation or translational repression. The maturation of hairpin transcript give rise to a 3p guide strand and 5p sister passenger strand. In general, only one species remains while the complementary species is degraded but in some cases, both strands can be produced allowing the silencing of specific sets of genes through base pairing to a minimal recognition sequence [7]. In this study, we describe a novel function for *miR-142* in the control of alveolar epithelial lineage formation.

*miR-142* is a major regulator of cell fate decision during organogenesis [8]. We previously reported that morpholino-based in vitro knockdown of *miR-142-3p* in the embryonic E11.5 lung led to decreased proliferation and premature differentiation of smooth muscle cell progenitors. Functionally, *miR-142-3p* positively regulates  $\beta$ -catenin signaling via targeting *Adenomatous polyposis coli* (*Apc*), a gene encoding an essential component of the  $\beta$ -catenin (Ctnnb1) degradation complex. Deletion of *Apc* or the ectopic expression of a stable form of  $\beta$ -catenin in the mesenchyme, which led to a rescue of the proliferation and differentiation defects previously observed upon silencing of *miR142-3p*, further validates *Apc* as a functional target downstream of *miR-142-3p* [9]. Interestingly, *miR-142-5p* has been reported to target *Ep300*, a positive regulator of  $\beta$ -catenin signaling [10, 11]. We previously reported the simultaneous upregulation of the negative  $\beta$ -catenin regulator *Apc* and the positive  $\beta$ -catenin regulator *Ep300* in *miR-142* KO E18.5 lungs. This was associated with increased  $\beta$ -catenin signaling in both the epithelium and mesenchyme [12]. Therefore, one reasonable possibility is that, in the context of the *miR-142* KO, *Ep300* is overriding the effect of *Apc* on  $\beta$ -catenin signaling.

We have deployed both in vivo gain and loss of function approaches for *miR-142* to study its role in alveolar epithelial lineage formation. Using FACS-isolated AT2 cells from mutant and control lungs, we carried out gene arrays to determine the corresponding transcriptional changes. An in vitro lung explant culture model allowing alveolar epithelial differentiation was used to monitor the status of *miR-142* expression. In this model, the effect of morpholino-based knockdown of *miR-142* on alveolar lineage formation was also characterized. Pharmacological blockade of *Ep300*/ $\beta$ -catenin interaction with IQ-1 and *Kras*/*Erk* signaling with SCH772984 was carried out. Our results suggest that a glucocorticoid-*miR-142*-*Ep300*- $\beta$ -catenin signaling axis is in place to control pneumocyte maturation.

## Results

### Enhancement of alveolar epithelial lineage formation via the activation of the glucocorticoid pathway leads to decreased *miR-142* expression

We previously reported that *miR-142-3p* and *-5p* are expressed in both the epithelium and the mesenchyme at E18.5 [12] suggesting that in addition to its reported role in the mesenchyme [9], *miR-142* could also play a function in the epithelium. We hypothesized that *miR-142* could control alveolar epithelial lineage formation during lung development. First, we took advantage of a previously reported in vitro model where activation of the glucocorticoid receptor pathway with dexamethasone increases alveolar epithelial lineage formation [13]. Treatment of E14.5 embryonic lungs grown in vitro for 4 days with dexamethasone (Fig. 1a) led to an increase in the expression of both AT1 (*Aqp5*, *Pdpn*) and AT2 markers (*Sftpc*) (Fig. 1c). The impact of Dex treatment on *Sftpc* at the protein level was confirmed by IF and western blot (Fig. 1e, f). Next, we investigated the impact of dexamethasone treatment on the expression of the specific *miR-142* isoforms. We observed a strong decrease in *miR-142-3p* and *-5p* expression upon Dex treatment (Fig. 1b) associated with a significant increase in *miR-142* targets *Apc*, *Ep300*, *Il6st* but not *Kras* (Fig. 1d) suggesting that some of the effects of dexamethasone on alveolar epithelial lineage formation could be due to decrease in *miR-142* expression. Downregulation of *miR-142* was already observed as early as after 12 h of culture (data not shown). The expression of the associated lncRNA, which is located in the *miR-142* locus [12], was not affected by dexamethasone.

### *miR-142-3p* and *miR-142-5p* are expressed in both the AT1 and AT2 lineages during lung development

To investigate whether both *miR-142-3p* and *miR-142-5p* are expressed specifically in the AT1 and AT2 cells, we performed fluorescence in situ hybridization specific to *miR-142-3p* and *-5p*, co-stained together with either *Sftpc* (AT2 marker) or *Pdpn* (AT1 marker) antibodies at three different time points (E16.5, E17.5, and E18.5) during alveolar lineage formation (Fig. 2a).

In our experimental conditions, *Pdpn* expression was not detectable by IF at E16.5 in contrast with the robust *Sftpc* expression at that stage. At E17.5 and E18.5, both *Sftpc* and *Pdpn* were detected. *miR-142-3p* and *5p* were expressed in *Sftpc*-positive cells at E16.5 (the alveolar progenitors) as well as in progressively differentiated AT2

cells at E17.5–E18.5. Interestingly, *miR-142* expression is mostly detected in the nuclear compartment rather than in the cytoplasm. This result was confirmed by qPCR for the two *miR-142* isoforms from the enriched cytoplasmic or nuclear fractions using adult mouse lungs (Fig. S1A, B). Finally, at E17.5 and E18.5, we clearly observed *Pdpn*-positive AT1 cells co-expressing *miR-142-3p* or *5p*. We further confirmed this observation using antibodies against *Hopx*, a well-defined AT1 marker (Fig. S1C). In addition, we noticed cells negative for *miR-142-3p* or *miR-142-5p* but positive for *Sftpc* or *Pdpn* and vice versa. This result supports previous observations made concerning the heterogeneity of the alveolar epithelial lineage in the adult lung [5, 14]. These results indicate that both miRs are expressed in the alveolar epithelium during development. Using FACS-based approach, with a combination of antibodies against *Cd45* and *Cd31* to exclude the hematopoietic and endothelial cells as well as *Epcam* antibodies for capturing epithelial (*Epcam*<sup>+ve</sup>) or mesenchymal (*Epcam*<sup>-ve</sup>) cells, we isolated resident epithelial and mesenchymal lung cells at E14.5, E16.5 and E18.5 and examined miR expression by qPCR (Fig. 2b). The validation of this approach was carried out for known epithelial (*Cdh1*, *Epcam*, *Fgfr2b*) or mesenchymal (*Fgf10*, *Acta2*, *Vimentin*) markers (Fig. S1D, E). The expression of *miR-142-3p* is higher in the mesenchyme than in the epithelium at E16.5 and E18.5 but not at E14.5. Interestingly, between E14.5 and E18.5, *miR-142-3p* expression in the epithelium progressively decreases while the expression of its bona fide targets *Apc*, *Ep300*, *Il6st*, and *Kras* was increased (Fig. 2e). Consistent with our previous observations, *miR-142-5p* was expressed at much lower level than *miR-142-3p* [9].

We also investigated the expression of these two microRNAs in E16.5, E17.5 and E18.5 FACS-isolated AT1 and AT2 cells (Fig. 2c). Alveolar epithelial cells were identified as *CD45*<sup>-ve</sup>/*CD31*<sup>-ve</sup>/*CD49*<sup>low</sup>/*Epcam*<sup>int</sup> and AT2 cells were identified as *CD45*<sup>-ve</sup>/*CD31*<sup>-ve</sup>/*CD49*<sup>low</sup>/*Epcam*<sup>int</sup> and *Pdpn*<sup>-ve</sup> while AT1 cells were identified as *CD45*<sup>-ve</sup>/*CD31*<sup>-ve</sup>/*CD49*<sup>low</sup>/*Epcam*<sup>int</sup> and *Pdpn*<sup>+ve</sup>.

At E16.5, the captured cells for the AT1 lineage (*Pdpn*<sup>+ve</sup>) are likely to contain, provided these cells have a biological significance, the putative bipotent progenitors [5, 15]. In addition, the captured cells for the AT2 lineage (*Pdpn*<sup>-ve</sup>) are mostly made of alveolar progenitors. For the AT1 lineage, *miR-142-3p* was expressed at similar level between E16.5 and E18.5. On the contrary, the expression of *miR-142-5p* increased as the formation of the AT1 lineage progressed. Similar expression patterns for *miR-142-3p* and *5p* were observed in the formation of the AT2 lineage. Interestingly, we noted the higher enrichment of *miR-142-5p* in AT1 compared to AT2 cells at E18.5. Furthermore, data mining analysis on the expression of *miR-142* targets using the single cell AT1 and AT2 transcriptomic data at E18.5

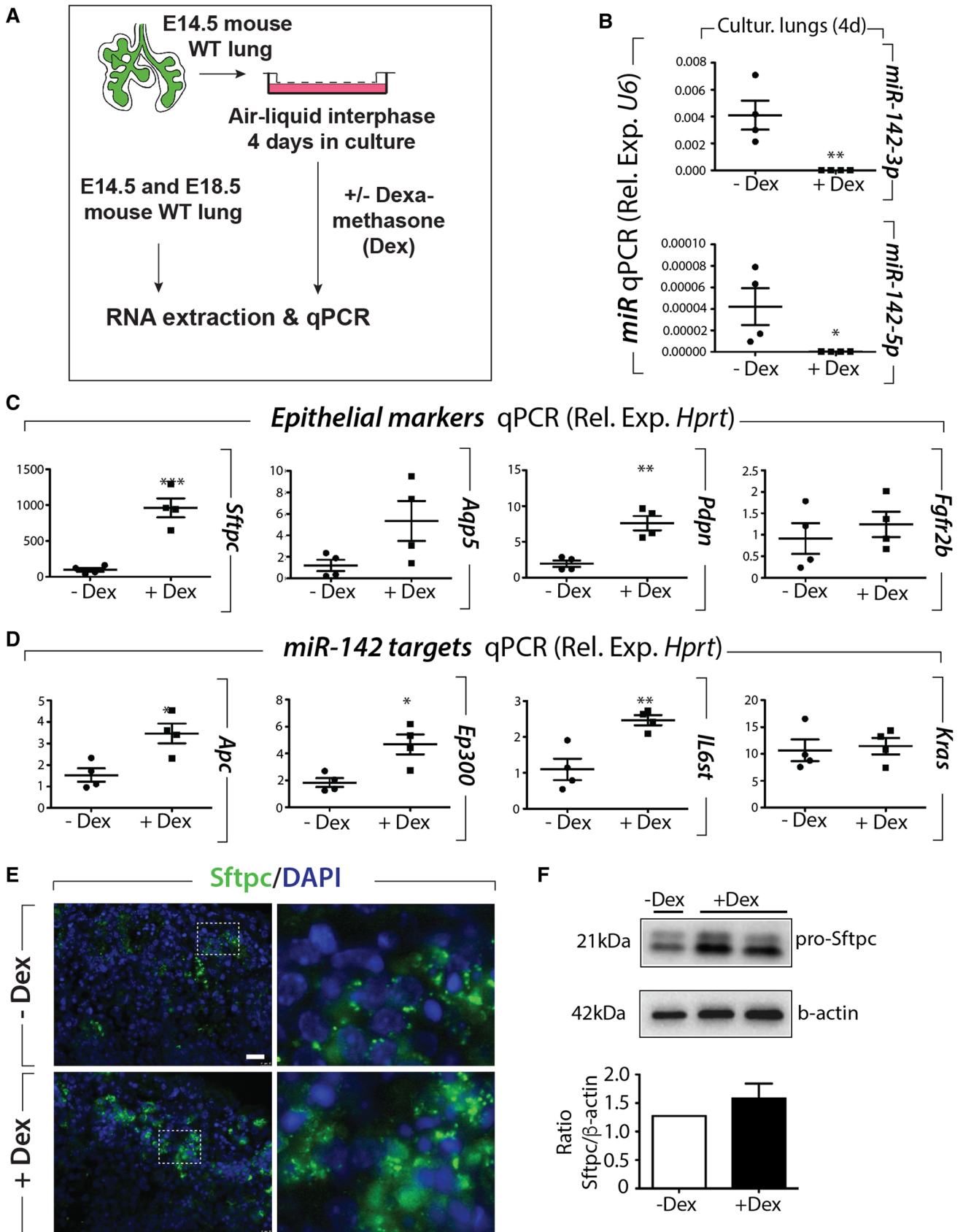




**Fig. 1** Effect of dexamethasone on E14.5 embryonic lung cultured in vitro for 4 days. **a** Experimental design ( $n=4$  for each  $\pm$  dexamethasone). **b** qPCR analysis showing the expression level of *miR-142-3p* and *miR-142-5p* as well as the expression of (**c**) *Sftpc*, *Aqp5*, *Pdpn* and *Fgfr2b*. **d** *Apc*, *Ep300*, *Il6st* and *Kras* on E14.5 lung explants grown for 4 days in presence of dexamethasone (100 nM), **e** IF staining for *Sftpc* on E14.5 lung explants cultured with and without dexamethasone (100 nM) for 4 days. **f** Representative western blot validating the increase in *Sftpc* expression in dexamethasone-treated lung explants. Scale bar in (**e**) low magnification: 16  $\mu$ m, high magnification: 4  $\mu$ m

previously published [5] was carried out (Fig. 2d). We have determined for each of the individual cells in the AT1 and AT2 pools, whether or not they express the different *miR-142* targets (*Apc*, *Ep300*). We have defined these cells as positive or negative for the expression of the target genes. For sake of simplification, we have not made a distinction in the “positive” cells between cells expressing high or low level of the target genes. We noticed that a higher number of individual cells in the AT2 pool expressed *Apc* and *Ep300* (7 out of 12 cells total analyzed and 5 out of 12 cells total analyzed, for *Apc* and *Ep300*, respectively) compared to AT1 (12 out of 41 cells total analyzed and 10 out of 41 cells total analyzed, for *Apc* and *Ep300*, respectively) (Fig. 2d). This supports our result that *miR-142* expression is low in AT2 compared to AT1 cells. Interestingly, a higher number of cells in the AT1 compared to AT2 pools expressed *Kras* (19/41 and 2/12, for AT1 and AT2, respectively) suggesting that *Kras* expression level is not regulated by *miR-142* in AT1 cells. *Il6st* was expressed by a low number of cells in the AT1 and AT2 pools (3/41 and 1/12, for AT1 and AT2, respectively). Altogether, the increase in these *miR-142* targets appears to occur more in AT2 than AT1, confirming the observed differential expression of *miR-142* in these cells. Therefore, it is logic to expect that the formation of the AT1 cells will be disrupted upon loss of *miR-142*.

### At the pseudoglandular stage of lung development, *miR-142* KO lungs display alteration in the morphology of the epithelial cells located at the tip but without major branching defects

To further explore the function of *miR-142* during lung development, we generated *miR-142* KO mice (Fig. 3a) leading to the inactivation of the *-3p* and *-5p* isoforms simultaneously [12]. No obvious macroscopic abnormalities in terms of branching were observed at E12.5 (Fig. 3b). This result was quite surprising as we previously reported that the knockdown of *miR-142-3p* using morpholino in E11.5 lungs grown in vitro led to impaired branching and loss of  $\beta$ -catenin signaling in the mesenchyme. The latter was associated with increased Adenomatous polyposis coli (*Apc*) expression and arrested proliferation [9]. The lack of obvious

branching phenotype in *miR-142* KO E12.5 lungs suggested that *miR-142-5p* could also play a functional role. *Apc* and *Ep300*, known targets for *miR-142-3p* and *miR-142-5p*, respectively, appeared to be upregulated at the protein level in KO lungs (Fig. 3c, d) while no significant change at the transcriptional level was observed (Fig. 3e). This could be explained by the fact that microRNAs do not act only at the level of the transcripts stability of the target genes but also at the translational level. In addition, in spite of elevated levels of  $\beta$ -catenin (*Ctnnb1*) mRNA (Fig. 3e), no significant changes of activated  $\beta$ -catenin ( $p^{S552}$ Ctnnb1) level in E12.5 *miR-142* KO compared to wild-type littermate controls was observed. Several possibilities for this discrepancy can be proposed. For example  $\beta$ -catenin protein degradation could be drastically increased at that stage in *miR-142* KO lungs. In addition, a disconnect between the levels of *Ctnnb1* at the transcriptional levels and at the protein level could also explain this lack of impact on  $\beta$ -catenin signaling at this early stage.

Further, in vitro knockdown experiments using morpholinos against *miR-142-3p* (*mo-3p*), *-5p* (*mo-5p*) or (*3p+5p*) (*mo-(3p+5p)*) indicated that simultaneous inactivation of both isoforms leads to the rescue of the branching defects reported upon *miR-142-3p* knockdown alone (Fig. S2 and [9]).

Careful examination of E12.5 *miR-142* KO lung epithelium, by immunofluorescence for E-cadherin (*Cdh1*), suggested a disruption in the epithelial cuboidal cell morphology, and acquisition of a round shape with the overall disorganization of the epithelial layer (Fig. 3b). Global transcriptomic analysis using gene arrays with RNA originating from the whole control and KO E12.5 lungs was also carried out. The heat map (Fig. 3f) shows sets of up- or down-regulated genes selected based on their  $p$  value in control and KO lungs ( $n=3$ ). KEGG gene set analysis indicated perturbations in pathways involved in regulation of actin cytoskeleton, focal adhesion and endocytosis as well as ECM receptor interaction. All these pathways, which have been shown to modulate epithelial integrity and maturation, may be involved in the observed phenotype. Interestingly, PI3K-Akt, Mapk, Ras, Hippo and Wnt signaling were also perturbed (Fig. 3f).

### The alveolar epithelial lineage is perturbed in E18.5 *miR-142* KO lungs

Macroscopic analysis of the E18.5 KO lungs indicated no obvious changes in terms of size or shape, when compared to wild-type littermates. Analysis of the microscopic phenotype by H&E staining ( $n=3$ ) also revealed no major structural abnormalities (Fig. 4a). Transcriptomic analysis between KO and control lungs at E18.5 indicated perturbation in the extracellular matrix-receptor interaction, focal

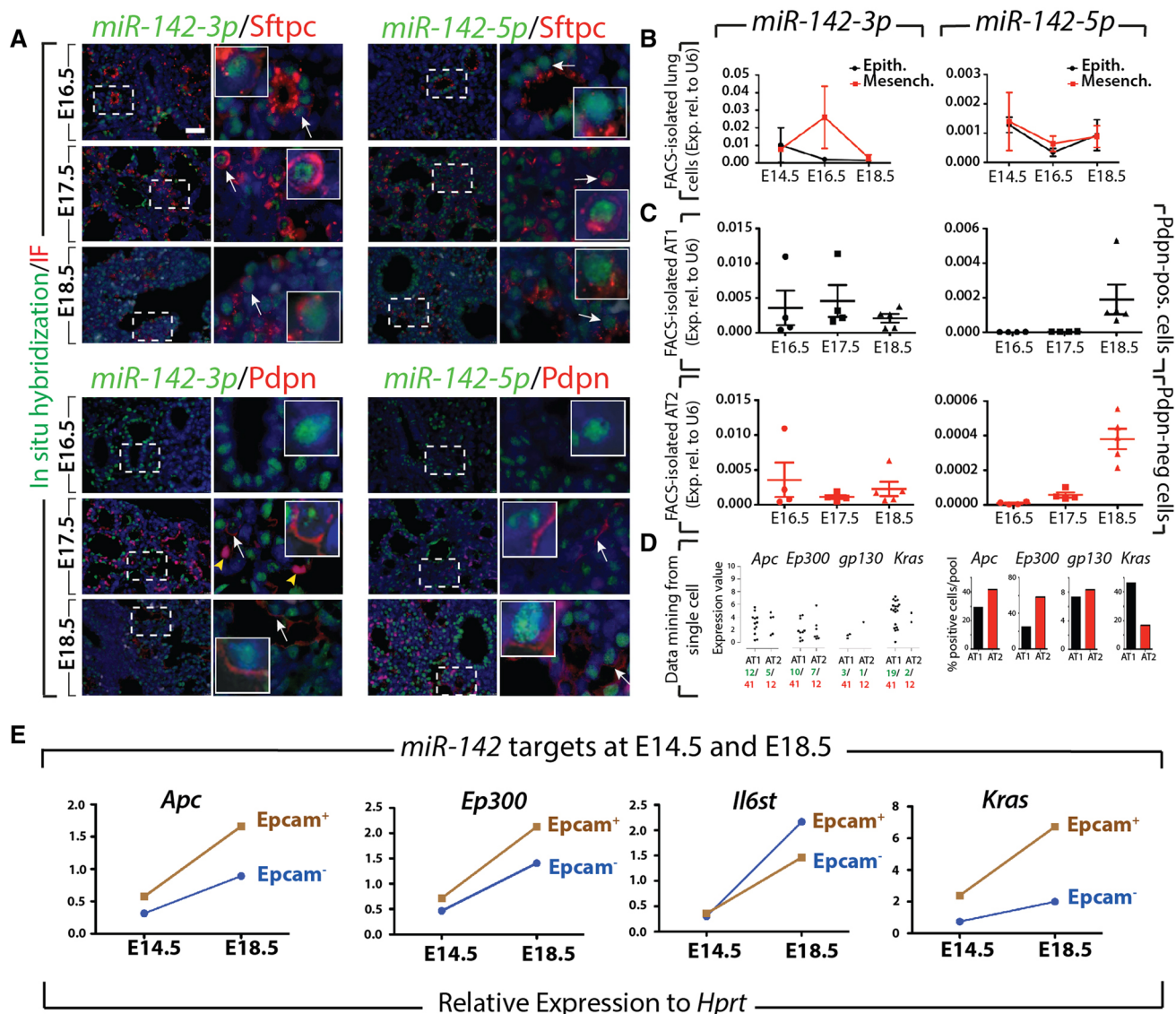


**Fig. 2** Gene expression analysis during lung development of *miR-142-3p* vs. *miR-142-5p*. **a** In situ hybridization of *miR-142-3p* or *5p* and co-immunofluorescence staining for either *Sftpc* (AT2 marker) or *Pdpn* (AT1 marker). High magnification insets for *Sftpc/miR-142-3p* and *-5p*-positive and *Pdpn/miR-142-3p* and *-5p*-positive cells in both WT embryos at 16.5, E17.5 and E18.5 are shown ( $n=3$  for each time point). **b** qPCR on FACS-isolated lung epithelium and mesenchyme at E14.5, E16.5 and E18.5 ( $n=4$  for each time point).

**c** qPCR on FACS-isolated AT1 and AT2 cells at E16.5, E17.5 and E18.5 ( $n=4$  for each time point). **d** Mining of single cell transcriptomic data for AT1 and AT2 cells at E18.5 (using data from [5]). **e** Expression analysis of *miR-142* targets *Apc*, *Ep300*, *Il6st* and *Kras* in the mesenchyme as well as in the epithelium ( $n=3$ ). *Hprt* is used as a house-keeping gene. Scale bar in **a** low magnification: 30  $\mu\text{m}$ , high magnification: 8  $\mu\text{m}$ . White arrows indicate cells with positive signals whereas yellow arrowheads show background signals

adhesion, hematopoietic cell lineage and Wnt signaling (Fig. S3). Further validating our previous findings [12], we observed a significant increase in the level of expression of *Apc*, *Ep300*, and *Il6st* in E18.5 KO lungs in mRNA level by qPCR (Fig. 4b). We further confirmed at the protein level by immunofluorescence staining the upregulation of *Apc* (Fig. 4c) and *Ep300* (Fig. 4d) with an increased level of activated  $\beta$ -catenin ( $p^{S52}\text{Ctnnb1}$ ) compared to the control lungs, suggesting increased Wnt signaling (Fig. 4e). However, the expression of Wnt components *Lef1* and

*Ctnnb1* were not significantly affected (Fig. 4b). Finally, we observed an increased p-Erk expression (Fig. 4f), correlating with increased *Kras* mRNA levels (Fig. 4b). Gene expression analysis by qPCR on the whole lung indicated that the AT2 marker, *Surfactant protein C* (*Sftpc*) was upregulated in KO vs. control lungs ( $p=0.0074$ ,  $n=3$ ) (Fig. S4C). Both FACS and immunofluorescence confirmed an increase in the expression level of *Sftpc* in the KO (Fig. 4g, h). The expression of the AT1 marker Podoplanin (*Pdpn*) ( $p=0.06$ ,  $n=3$ ), the Club cell marker *Scgb1a1* and the

basal cell marker *p63* were not significantly changed (Fig. S4C). Flow cytometry analysis using Epcam, CD49f, Pdpn antibodies showed an increase in the percentage of AT2 cells ( $84.9\% \pm 0.2\%$  vs.  $79.8\% \pm 1.04\%$  in KO vs. control, respectively,  $p = 0.002$ ,  $n = 3$ ), and a decrease in the percentage of AT1 cells ( $9.05\% \pm 0.68\%$  vs.  $12.3\% \pm 0.66\%$  in KO vs. control, respectively,  $p = 0.004$ ,  $n = 3$ ) (Fig. 4g). The increase in Sftpc-positive cells (AT2) and decrease in Hopx-positive cells (AT1) in KO vs. WT lungs were confirmed by IF (Fig. 4h,  $n = 3$ ). Analysis of Ki67 immunoreactivity, in the alveolar epithelial layer of control and KO lungs at E18.5, indicated no changes in epithelial proliferation (Fig. S4D). Furthermore, by flow cytometry analysis no changes in the percentage of Epcam-positive cells (Epcam<sup>+</sup>) were observed (Fig. S4A), suggesting that the loss of *miR-142* is not affecting overall, epithelial proliferation. We also carried out using gene arrays, the transcriptomic analysis of isolated AT2 cells between KO and control lungs (Fig. 4i). Our KEGG analysis indicated that the metabolic pathways, endocytosis, focal adhesion, actin cytoskeleton regulation, peroxisome and Hippo signaling were affected.

Next, we explored the status of Fibroblast growth factor 10 (*Fgf10*) signaling, a key pathway reported to influence alveolar epithelial lineage formation [16, 17]. We found that the expression of *Fgf10* was not changed but a very significant increase in the expression of its receptor, *Fgfr2b*, in KO vs. control lungs ( $p = 0.0018$ ) was observed (Fig. S5A). The protein expression levels were in line with the gene expression levels (Fig. S5B). Analysis of *Sprouty2* and *Etv5*, two previously reported *Fgf10* downstream targets [18, 19], showed no significant difference between control and KO lungs (Fig. S5A), suggesting that *Fgf10* signaling per se was not affected.

In conclusion, we demonstrate increased AT2/AT1 cell number ratio in KO vs. control lung.

### Impact of cell autonomous overexpression of *miR-142* in alveolar progenitors

The expression of *miR-142* in the epithelium as well as the epithelial alveolar lineage phenotype upon global loss of function of *miR-142* suggested that *miR-142* could play a cell autonomous role in the epithelium. To test this possibility, we generated a knock in of the *LoxP-Stop-LoxP-miR142* cassette in the *Rosa26* locus (*Rosa26<sup>miR-142/miR-142</sup>*). We crossed the *Rosa26<sup>miR-142/miR-142</sup>* mice with *Sftpc<sup>CreERT2/+</sup>; Tomato<sup>flox/flox</sup>* mice, to generate control *Sftpc<sup>+/+</sup>; Rosa26<sup>miR-142/+</sup>; Tomato<sup>flox/+</sup>* and gain of function (GOF) *Sftpc<sup>CreERT2/+</sup>; Rosa26<sup>miR-142/+</sup>; Tomato<sup>flox/+</sup>* embryos. This Cre-based recombination, allows an irreversible activation of *miR-142* expression in the epithelium. The expression of *miR-142* was induced with tamoxifen IP injection at E14.5 and E15.5. The resulting lung phenotype was analyzed at

E18.5 (Fig. 5a). Experimental lungs were detected via the expression of red fluorescent protein (RFP) in the epithelium and confirmed by genotyping. Validating our approach, we found increased *miR-142-3p* ( $p = 0.0024$ ) and *-5p* ( $p = 0.0004$ ) expression in GOF vs. control lungs (Fig. 5b). FACS analysis of CD49f<sup>low</sup>/Epcam<sup>int</sup> alveolar epithelial cells as well as AT1 (Pdpn<sup>+</sup>) and AT2 (Pdpn<sup>-</sup>) cells indicated no change in the percentage of alveolar epithelial cells (over total cell population). However, a significant decrease in the percentage of AT2 cells ( $82.4\% \pm 1.24\%$  vs.  $86.6\% \pm 0.99\%$  in GOF vs. control,  $p = 0.004$ ,  $n = 4$ ) and an increase in the percentage of AT1 cells ( $10.6 \pm 0.88\%$  vs.  $8.7 \pm 0.38\%$  in GOF vs. control,  $p = 0.001$ ,  $n = 4$ ) was observed (Fig. 5c). Immunofluorescence staining for Sftpc and Hopx indicated a decrease in AT2 and increase in AT1 cell number in E18.5 GOF embryos compared to control (Fig. 5d). The general pattern and level of expression of Pdpn was also increased in GOF vs. control lungs supporting the increase in AT1 cell number in GOF lungs by FACS (data not shown). Quantification of the percentage of [Sftpc<sup>+</sup>; Pdpn<sup>+</sup>] cells over total number of cells (Fig. 5d) also indicates a trend towards an increase in GOF vs. control lungs ( $3.18\% \pm 0.74\%$  vs.  $1.16\% \pm 0.08\%$ ,  $p = 0.06$ ).

Next, we carried out gene arrays from E18.5 control and GOF FACS-isolated AT2 cells ( $n = 3$ , Fig. 5e). KEGG analysis indicates that G-coupled protein-mediated olfactory transduction, metabolic pathways, and RNA degradation were affected.

In conclusion, gain of *miR-142* expression in alveolar epithelial cells led to a decreased AT2/AT1 cell ratio.

### Loss of *miR-142* expression in vitro starting at E14.5 is sufficient to increase the AT2/AT1 cell ratio

As the *miR-142* KO lung phenotype (where both isoforms are deleted) is different from the phenotype observed upon silencing of *miR-142-3p* in vitro [9], it was important to validate our morpholino approach against *miR-142*. We carried out the simultaneous silencing of both isoforms (*miR-142-3p* and *miR-142-5p*) at E12.5 in vitro. The silencing of *miR-142-3p* was used as a positive control for our experiments. Our data indicate that the silencing of both isoforms has no impact on lung branching, a phenotype observed in vivo in the *miR-142* KO (Fig. S2A). Silencing only *miR-142-3p* leads to the impaired branching phenotype as previously reported [9]. qPCR data on the in vitro-cultured lungs indicated that silencing both isoforms led to the loss of expression of both *miR-142-3p* and *-5p*. Silencing only *miR142-3p* led to the loss of *miR-142-3p* but not *-5p* (Fig. S2B).

To evaluate the impact of *miR-142* loss of function at the time in which AT2 (*Sftpc*) and AT1 (*Pdpn*) cell markers arise, we performed in vitro treatment with morpholino specific for *miR-142-3p* and *-5p* on E14.5 lung explants and



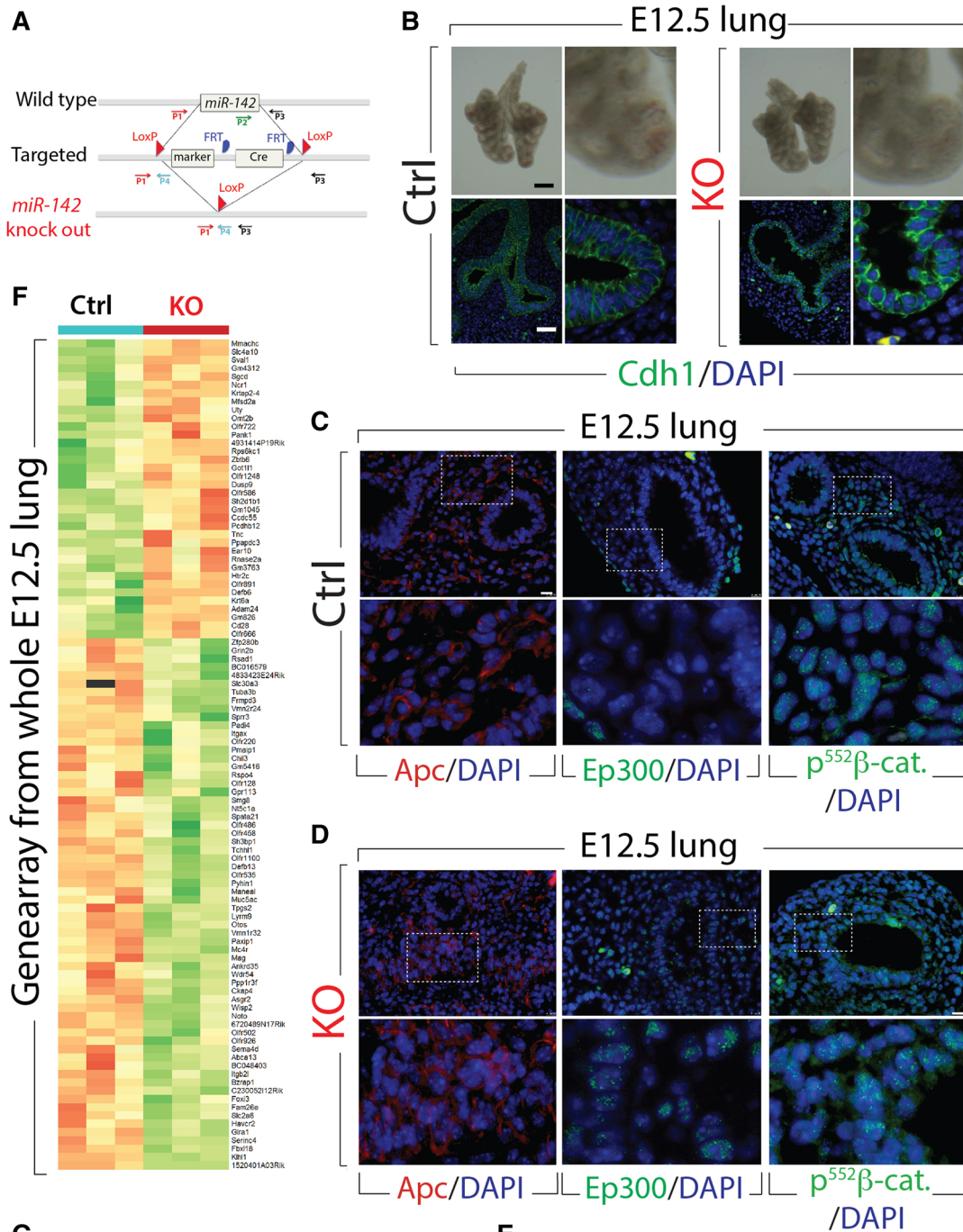




**Fig. 3** Analysis of the *miR-142* KO at E12.5. **a** Generation of the *miR-142* KO by homologous recombination. **b** Bright field picture and Cdh1 staining of control (WT) littermate and *miR-142* KO lungs at E12.5 (minimum  $n=3$ ). **c, d** Immunofluorescence staining for Apc, Ep300 and activated  $\beta$ -catenin ( $p^{S552}$ Ctnnb1) ( $n=3$ ) and **e** gene expression analysis of *miR-142* target genes by qPCR in E12.5 controls and *miR-142* KO lungs ( $n=3$ ). **f** Heat map of the most differentially expressed genes (according to their  $p$  values) between KO and control lungs at E12.5 ( $n=3$ ). **g** Corresponding KEGG pathway analysis. Scale bar for bright field: low mag: 400  $\mu$ m, high mag: 100  $\mu$ m. Scale bar for immunofluorescence: low mag: 40  $\mu$ m, high mag: 10  $\mu$ m

cultured them for 4 days (Fig. 6a). This approach allowed analyzing the effect of *miR-142* LOF at a time when early alveolar progenitors have yet to differentiate into AT1 and AT2 cells [5]. We observed a significant decrease in the expression of *miR-142-3p* and *-5p*, respectively (Fig. 6b). Treatment with both morpholinos together (*mo*-(*3p+5p*)) led to the simultaneous knockdown of both *miR-142* isoforms (Fig. 6b). The decrease in the expression of these *miRNAs* was further confirmed by upregulation of their respective target genes such as *Apc*, *Ep300* and *Kras* (Fig. 6c). Interestingly, the attenuation of *miR-142-3p* and/or *-5p* led to the increase in *Sftpc* expression while decreasing the expression of *Pdpn* (Fig. 6d). In accordance with our in vivo data, FACS analysis of AT2 and AT1 cells in these lungs grown in vitro demonstrated an increase in the percentage of AT2 ( $14.8\% \pm 1.33\%$  vs.  $7.9\% \pm 4.8\%$  in *mo*-(*3p+5p*) vs. *Scramble*, respectively,  $p=0.049$ ,  $n=4$ ) and a decrease in AT1 ( $0.86\% \pm 0.2\%$  vs.  $2.8\% \pm 1.1\%$  in *mo*-(*3p+5p*) vs. *Scramble*, respectively,  $p=0.01$ ,  $n=4$ ) (Fig. S6). The phenotype resulting from the knockdown of *miR-142* in vitro using morpholinos was validated in *miR-142* KO and WT lungs grown in vitro (Fig. S7). In particular, we found that *miR-142* KO lungs grown in vitro display increased *Sftpc* expression compared to the corresponding control. Therefore, our results demonstrate that in vitro knockdown of *miR-142* recapitulates the in vivo phenotype in terms of AT2/AT1 ratio. This result reinforces the concept that the observed phenotype is due to a direct effect of perturbing *miR-142* signaling, rather than to secondary effects due to prolonged absence of *miR-142*.

### Blockade of Ep300/ $\beta$ -catenin (Ctnnb1) in vitro using the pharmacological inhibitor IQ-1 prevents *miR-142*-LOF-induced increase in *Sftpc*

To identify the molecular mechanism responsible for the perturbation of alveolar lineage formation by silencing *miR-142*, the activity of its downstream targets were modulated. We employed the pharmacological inhibitor IQ-1 (blocks Ep300/ $\beta$ -catenin interaction) and SCH772984, a specific inhibitor of Erk1/2 (inhibits Kras/Erk signaling). Treatment with IQ-1 (10  $\mu$ m) and SCH772984 (10  $\mu$ m) on E14.5 lung

explants for 4 days showed that both inhibitors were efficient in reducing *Sftpc* expression (Fig. 6e, h, j) but did not alter the level of *Pdpn* expression (data not shown). It is not clear whether this effect is *miR-142* dependent or independent. Given the fact that *miR-142* silencing enhances *Sftpc* expression compared to scramble, we investigated the relevance of the Erk and Ep300/ $\beta$ -catenin signaling downstream of *miR-142* using these inhibitors in our lung explant model (Fig. 6f).

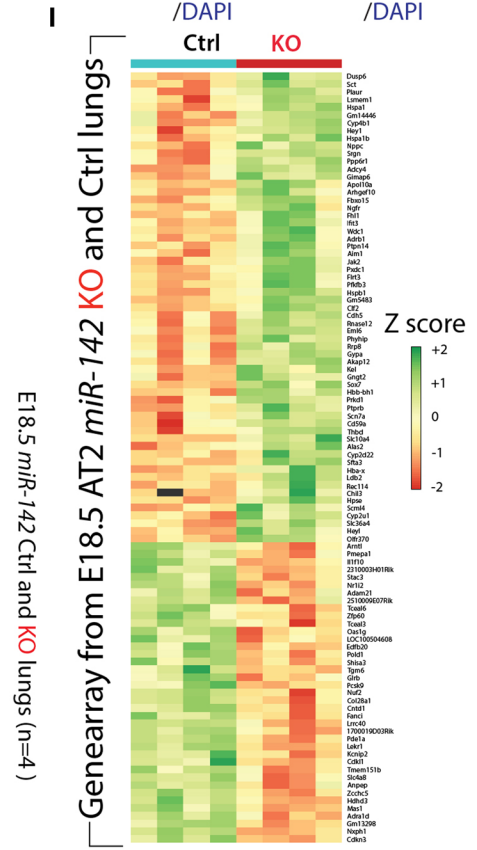
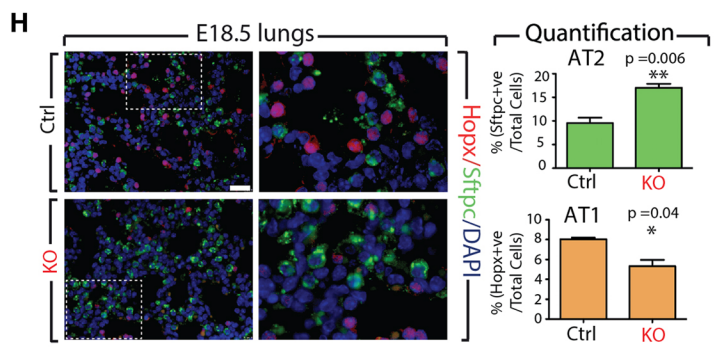
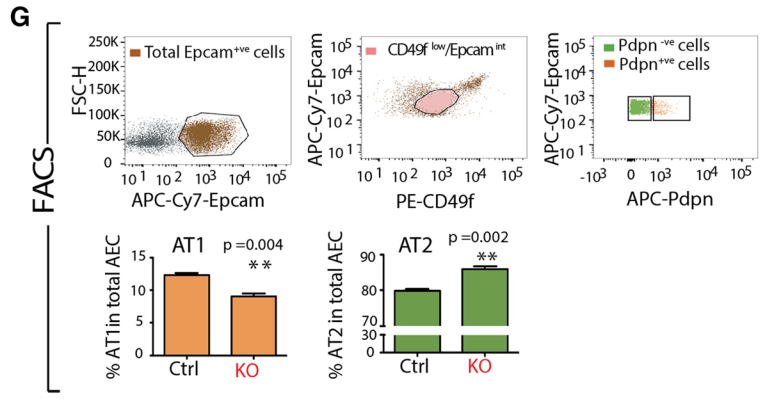
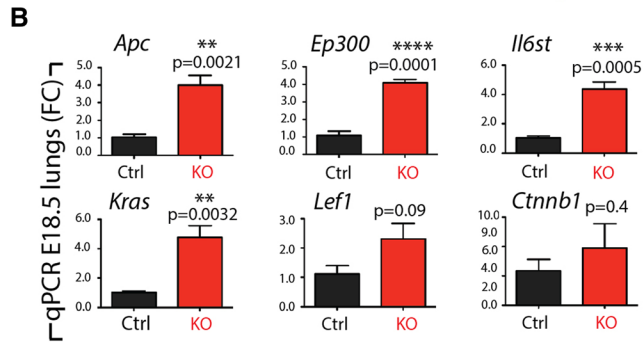
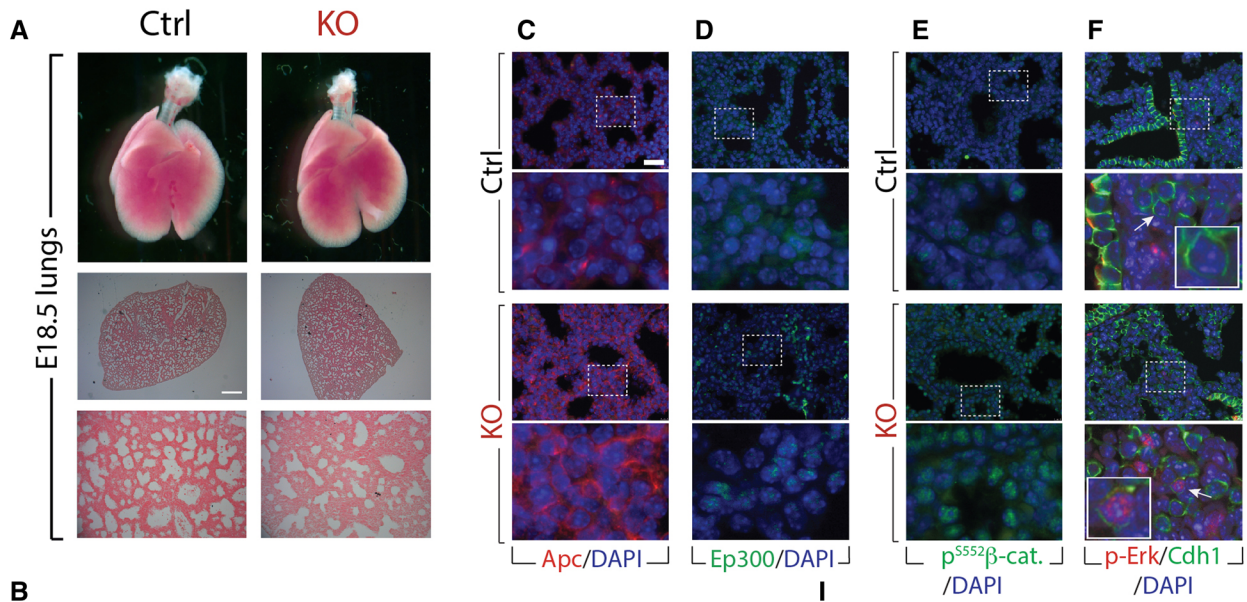
In presence of IQ-1, silencing *miR-142* in E14.5 lung explants were not able to rescue the increased expression of *Sftpc* phenotype being observed in *miR-142* knockdown alone (Fig. 6g, h). On the other hand, silencing *miR-142* in SCH772984 (Erk inhibitor) treated E14.5 lung explants led to a moderate but significant increase in the expression of *Sftpc* compared to the control scramble treated with Erk inhibitor (Fig. 6i, j). These results suggest that Ep300/ $\beta$ -catenin rather than Kras/Erk signaling is downstream of *miR-142* to control *Sftpc* expression.

Validating our in vitro approach using morpholinos, KO lungs grown in vitro showed increased *Sftpc* expression compared to the corresponding control wild-type lung (Fig. S7A) confirming the results obtained in vivo. In addition, KO lungs ( $n=3$ ) grown in vitro in presence of Erk inhibitor displayed increased *Sftpc* expression compared to the corresponding control wild-type lungs (also grown with Erk inhibitor) ( $n=3$ ) (Fig. S7B). Further supporting our in vitro morpholino-based approach, KO lungs ( $n=4$ ) grown in vitro in presence of IQ1 displayed no change in *Sftpc* expression compared to the corresponding control wild-type lungs (also grown with IQ1) ( $n=3$ ) (Fig. S7C).

## Discussion

The mechanisms regulating alveolar epithelial cells proliferation and differentiation as well as the advancement of distinct lung progenitor cells towards given mature alveolar cell types are poorly understood [20–22]. Recently, studies based on the use of cell-specific markers as well as single cell transcriptomic of the epithelium during lung development suggested that AT1 and AT2 cells derive from common bipotent progenitor cells [5, 15]. The biological relevance of the BP model as progenitor for AT1 and AT2 is still unclear. Alternatively, *Sftpc*-positive alveolar progenitors could progressively differentiate into either AT1 or AT2. The differentiation towards the AT1 lineage would require losing *Sftpc* expression/AT2 markers and acquiring AT1 markers.

Interestingly, at E16.5, alveolar progenitors (Epcam<sup>+ve</sup> Cd49f<sup>+ve</sup>) can be subdivided by FACS into two populations based on the expression of *Pdpn*. We propose that *Pdpn*<sup>+ve</sup> cells are alveolar progenitor cells differentiating towards the AT1 lineage and expressing, therefore, *Pdpn*; these cells can



KEGG analysis at E18.5 (KO vs. Ctrl)

KEGG name	n GenesInSet	n expr. genes	-log(p)
Metabolic pathway	1224	1144	15.54
Endocytosis	272	262	9.71
Focal adhesion	202	193	6.59
actin cytoskeleton	215	204	5.49
Peroxisome	83	80	4.97
Oxidative phosphor.	116	114	4.92
Tight junction	139	134	4.62
Hippo signaling	153	148	4.26

**Fig. 4** Analysis of the alveolar epithelial lineage phenotype of the *miR-142* control and KO lungs at E18.5. **a** Bright field pictures, H&E staining of control and *miR-142* KO lungs at E18.5 ( $n=3$ ). **b** Gene expression analysis of *miR-142* target genes by qPCR in E18.5 controls and *miR-142* KO lungs ( $n=3$ ). Immunofluorescence staining for **c** Apc, **d** Ep300, **e** activated  $\beta$ -catenin ( $p^{S552}$ Ctnnb1) and **f** p-Erk/Cdh1 ( $n=3$  each). **g** FACS of control and *miR-142* KO lungs ( $n=3$ ) using Epcam, Cd49f and Pdpn antibodies. Quantification of AT1 (Cd49<sup>low</sup>; Epcam<sup>int</sup>, Pdpn<sup>+ve</sup>) and AT2 (Cd49<sup>low</sup>; Epcam<sup>int</sup>, Pdpn<sup>-ve</sup>) cells. **h** Hopx/Sftpc/DAPI IF staining in control and KO E18.5 lungs and the corresponding quantification of AT1 and AT2 cells ( $n=3$ ). **i** Heatmap of the most differentially expressed genes (according to their  $p$  values) between AT2-isolated cell from KO and control lungs at E18.5 ( $n=4$ ) and corresponding KEGG pathway analysis. Scale bar **a** low mag: 125  $\mu$ m, high mag: 31  $\mu$ m; scale bar **c-f**: low mag: 25  $\mu$ m, high mag: 6  $\mu$ m. Scale bar **h**: low mag: 20  $\mu$ m, high mag: 5  $\mu$ m

either be BP cells (Sftpc<sup>+ve</sup> and Pdpn<sup>+ve</sup>) or simply alveolar progenitor cells which have acquired Pdpn and also lost Sftpc. On the other hand, we expect the Pdpn<sup>-ve</sup> cells to be the alveolar progenitor cells differentiating towards the AT2 lineage.

The fact that we can detect two populations (Pdpn<sup>+ve</sup> and Pdpn<sup>-ve</sup>) at E16.5 indicates that the bipotent mode is not widely applicable (otherwise we should only detect the Pdpn<sup>+ve</sup> cells). It is likely that only a small proportion of the alveolar progenitors (Sftpc<sup>+ve</sup>) acquire Pdpn expression at E16.5 to become bipotent progenitor cells. The overall majority of the alveolar progenitors express only Sftpc. Again, in the future, lineage tracing experiments for the BP should be carried out to elucidate their exact contribution to the AT1 and AT2 lineages.

Using a constitutive KO mouse model, we report that in the absence of *miR-142* (abolishing both the  $-3p$  and  $-5p$  strands), there is an relative increase of AT2 and a decrease in AT1 cell number (leading to an increase in the AT2/AT1 cell number ratio). Examination of the KO versus control lungs at E18.5, revealed enhanced expression of the *miR-142* targets *Apc* and *Ep300*, associated with increased  $\beta$ -catenin and p-Erk signaling. Supporting a cell autonomous function for *miR-142* in the epithelium, increased *miR-142* from E14.5 to E18.5 in alveolar progenitor cells led to the opposite effect. Interestingly, no changes in the number of Epcam or Ki-67-positive cells were observed suggesting a direct impact of *miR-142* in epithelial cell differentiation. Activation of the glucocorticoid pathway in an in vitro alveolar epithelial lineage differentiation assay was sufficient to achieve decreased *miR-142* expression and enhanced *Sftpc* expression. Morpholino-based knockdown of *miR-142* was sufficient to induce *Sftpc*, decrease *Pdpn* expression and increase AT2/AT1 cell number ratio. In addition, *Apc*, *Ep300* and *Kras* expression were up-regulated. Pharmacological inhibition of Ep300/ $\beta$ -catenin but not the Kras/Erk signaling completely prevented *miR-142* morpholino-based increase in *Sftpc* expression. These results suggest that a

glucocorticoid-*miR-142*-Ep300 signaling axis controls the differentiation of alveolar progenitors and maintains the balance between AT1 and AT2 cells.

Recently, we showed that Fgf10 might represent a crucial molecule, controlling the differentiation of alveolar epithelial progenitor cells towards the AT2 lineage [16]. Using *Fgf10* heterozygous (*Fgf10*<sup>+/-</sup>) lungs, we demonstrated a decrease in the AT2/AT1 cell ratio as well as surfactant production impairment in newborn pups. These changes are associated with a fully penetrant lethal phenotype after hyperoxia injury. Furthermore, a defect in epithelial differentiation and proliferation was observed in *Fgf10* hypomorphic lungs showing impairment in AT2 lineages [17]. While we cannot exclude changes in components of Fgf10 signaling in the *miR-142* KO, *Fgf10* as well as its downstream targets *Etv5* and *Sprouty2* were unchanged in our model. Furthermore, the fact that pharmacological inhibition of Ep300/ $\beta$ -catenin but not the Kras/Erk signaling completely prevented *miR-142* morpholino-based increase in *Sftpc* expression, suggests a prominent role for Wnt signaling downstream of *miR-142*.

Recently, a role for *histone deacetylase 3* (*Hdac3*) in the spreading of AT1 cells and lung sacculation was reported. It was shown that *Hdac3* expressed in alveolar progenitors represses the expression of *miR-17-92* [23]. *miR-142* does not appear to impact the spreading of AT1 cells as no such defects were detected at E18.5 or postnatally (data not shown). In addition, the adult KO lungs are functional and appear histologically normal ([12] data not shown). There is no evidence so far of an organized cross-talk between *miR-142* and *miR-17-92* during the late phase of lung development. During early development *miR-17-92* was shown to modulate Fgf10-Fgfr2b signaling by specifically targeting *Stat3* and *Mapk14*, hence regulating Cdh1 expression. Cdh1 expression level in turn fine-tunes Ctnnb1 signaling in the epithelium, which is critical for epithelial bud morphogenesis triggered by Fgf10 [24]. Interestingly, mutant lungs with specific deletion of *Hdac3* in the mesenchyme also display impairment of AT1 differentiation, correlating with decreased Ctnnb1 signaling in the epithelium. Rescue of Ctnnb1 signaling in the mutant lung partially rescues AT1 cell differentiation defects [25]. Again, as Ctnnb1 signaling is increased in the *miR-142* KO epithelium, it is very unlikely that this leads to the perturbation of AT1 differentiation, conclusion that is supported by our analysis.

To identify the molecular mechanism involved in the regulation of alveolar epithelial phenotype by *miR-142*, we employed a well-established model to activate glucocorticoid signaling using dexamethasone to stimulate the maturation of alveolar cells into functional AT1 and AT2 cells [13, 26]. Interestingly, we noted a reduced expression of *miR-142-3p* and *miR-142-5p* in lung explants treated with glucocorticoid agonists, suggesting reduced level of *miR-142*



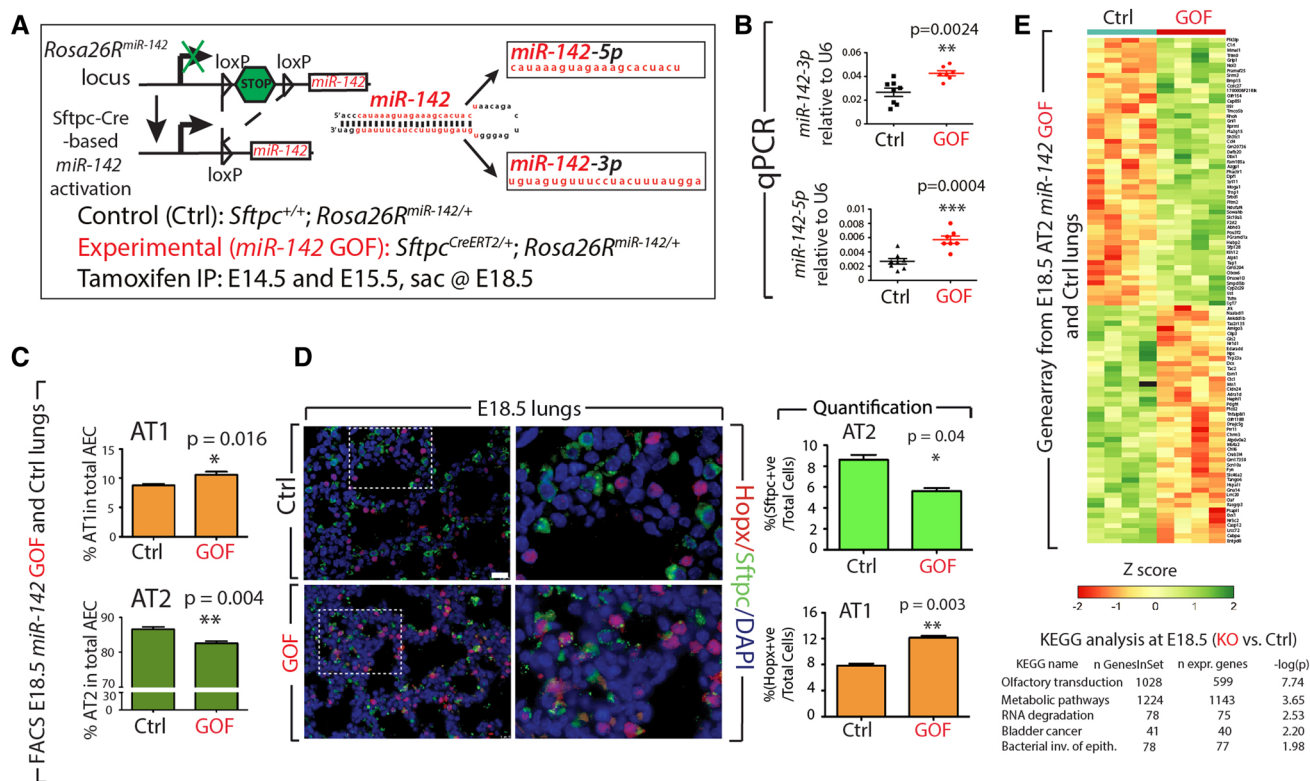


**Fig. 5** Analysis of the alveolar epithelial lineage phenotype of the *miR-142* gain of function (GOF) and littermate control lungs at E18.5. **a** *LoxP-Stop-LoxP-miR-142* knock in mice (in the *Rosa26* locus) are crossed with *Sftpc<sup>CreERT2</sup>* mice. Cre activation in the alveolar epithelial progenitor cells following tamoxifen IP injection to pregnant females at E14.5 and E15.5 leads to *miR-142* overexpression in these cells. Lungs are then analyzed at E18.5. **b** Validation of *miR-142-3p* and *-5p* overexpression in E18.5 GOF and control litter-

mate lungs. **c** FACS analysis of control and GOF E18.5 lungs ( $n=4$ ) for total Epcam, AT1 and AT2 cells. **d** *Hoxp/Sftpc/DAPI* IF staining in E18.5 GOF and control littermate lungs and the corresponding quantification. **e** Heatmap of the most differentially expressed genes (according to their  $p$  values) between AT2-isolated cell from GOF and control lungs at E18.5 ( $n=4$ ) and corresponding KEGG pathway analysis. Scale bar **d**: low mag: 16  $\mu$ m, high mag: 4  $\mu$ m

is required for the differential of alveolar epithelial cells. Furthermore, we demonstrated two equally important pathways downstream of *miR-142* playing an important role in the formation of the alveolar lineage. Ep300/ $\beta$ -catenin interaction has been shown to be one of the pathways involved in the differentiation of adult epithelial progenitors [27] as well as differentiation of embryonic stem cells and regulation of proximal–distal axis during lung development [28]. *Apc* and *Ep300*, two critical targets of *miR-142*, can control the  $\beta$ -catenin pathway. *Apc* is part of the degradation complex for  $\beta$ -catenin and is, therefore, a negative regulator of *Ctnnb1* signaling. Conversely, Ep300 binds to  $\beta$ -catenin and acts as a co-transcriptional activator. In vitro blockade of Ep300/ $\beta$ -catenin interaction with the use of IQ-1 showed complete downregulation of *Sftpc* expression, suggesting impairment in the alveolar epithelial lineage, while silencing *miR-142* in IQ-1-treated lung explants were unable to rescue the expression of the AT2 marker (Fig. 6g, h). The other pathway controlled by *miR-142* is the *Kras/Erk* pathway. A recent report indicated that *miR-142* is highly expressed in

undifferentiated mouse embryonic stem cells (mESCs) and downregulated in differentiated cells. It was also reported that overexpression of *miR-142* interrupted mESC differentiation. A double-negative feedback loop between *Kras/Erk* and *miR-142* levels has been suggested. Low level of *miR-142* triggers *Kras* and *Erk* phosphorylation, which in turn induces mESC differentiation and vice versa [29]. However, evidence suggests that *Kras* represses the formation of the alveolar lineage as forced activation of *Kras* in the distal lung epithelium in vivo suppresses the alveolar differentiation program [30]. In our in vitro model, lung explants treated with *Erk* inhibitor alone showed reduced *Sftpc* expression whereas *Erk* inhibitor treatment in combination with morpholino specific to *miR-142* showed a moderate increase in the *Sftpc* expression indicating a mild rescue in the alveolar lineage phenotype (Fig. 6i, j).

In conclusion, we report for the first time, an important role played by both isoforms of *miR-142* in alveolar epithelial lineage formation. We show that *miR-142* governs the formation of AT1 progenitors thereby controlling the AT2/AT1



cell number ratio. We propose that a glucocorticoid-*miR-142*-p300- $\beta$ -catenin signaling axis controls alveolar epithelial lineage formation (Fig. 6k).

## Materials and methods

### Mice

The *miR-142* KO mice on a pure C57BL6 background were previously generated [12]. *miR-142* heterozygous males and females were crossed to generate KO and WT littermate embryos at different stages. We also generated a knock in of *miR-142* in the *Rosa26R* locus. *Rosa26-LoxP-STOP-loxP-miR-142* (also known as *Rosa26R<sup>miR-142/miR-142</sup>*) mice were crossed with *Sftpc<sup>CreERT2/+</sup>* mice (kind gift from Dr. Chapman) to generate control (*Sftpc<sup>+/+</sup>; Rosa26<sup>miR-142/+</sup>*) and experimental (*Sftpc<sup>CreERT2/+</sup>; Rosa26R<sup>miR-142/+</sup>*) embryos. Pregnant females were injected with tamoxifen IP (0.1 mg/g of mouse) at E14.5 and E15.5 and collected at E18.5. Animal experiments were approved by the Federal Authorities of Animal Research of the Regierungspräsidium Giessen, Hessen, Germany with approved protocol numbers 405\_M, 423\_M, G 47/2017 and G54/2017. Animal protocols for the use of genetically modified animals were approved by Wenzhou University/Wenzhou Medical University animal care and use committee.

### Quantitative real-time PCR analysis

Briefly, total RNA from embryonic lungs were extracted and used for cDNA synthesis. RT-PCR for mRNA was carried out using Quantitative Reverse Transcription kit (205314; Qiagen) and Taqman MicroRNA Reverse Transcription kit (4366597; Applied Biosystem) was used in RT-PCR for miRNA. In both cases, reactions were assembled following the manufacturer's recommendations. qPCR was performed on a Light Cycler 480 system (Roche Applied Science). The TaqMan microRNA assay (Applied Biosystem) was used for screening the differential expression of miRNAs whereas SYBR Green (Platinum SYBR Green qPCR SuperMix-UDG Invitrogen) was used for the analysis of mRNA expression. *U6* and *Hprt* (Hypoxanthine phosphoribosyl transferase 1) were used as a reference for normalization of miRNA and mRNA, respectively. Results were collected from at least three lung samples and each reaction was run in triplicate. Primers for *miR142-3p*, *miR142-5p* and *U6* were obtained from Applied Biosystems.

### In situ hybridization and immunofluorescence staining

Freshly isolated lungs were washed in PBS, then fixed in 4% PFA, gradually dehydrated in ethanol, impregnated with

xylene, embedded in paraffin and sectioned into 5  $\mu$ m slices on poly-L-lysine-coated slides. Antigen retrieval was performed by treating the sample with Proteinase K for 1 min at 37 °C. The slides were blocked 2 times 5 min with Dako (DAB Emission + Dual Linksystem HRP, Life Technologies) and then incubated with digoxigenin-labeled LNA probes (Exiqon, miRCURY LNA Detection probe, Vedback, Denmark) specific for *miR142-3p* and *miR142-5p* and Anti-Digoxigenin-POD, Fab fragments (11207733910; Roche Diagnostics) were used to detect the signal by in situ hybridization.

For immunofluorescence staining, the slides were deparaffinized, blocked with 3% bovine serum albumin (BSA) and 0.4% Triton X-100 in Tris-buffered saline (TBS) at room temperature (RT) for 1 h and then incubated with primary antibodies against Apc (ab15270, Abcam; 1:250), phospho-S<sup>552</sup>- $\beta$ -catenin (9566, Cell Signaling; 1:250), Ep300 (sc-585, Santa Cruz; 1:250) and p-Erk (4376, Cell Signaling; 1:250), Sftpc (AB3786, Millipore; 1:500), Cdh1 (610181, BD Trans. Lab; 1:250), Fgfr2-BEK (sc-122, Santa Cruz; 1:250), Pdpn (8.1.1, DSHB; 1:250), Hopx (HPA030180, Atlas antibodies, 1:300) at 4 °C overnight. After incubation with primary antibodies, slides were washed three times in TBST (Tris buffer saline + 0.1% Tween 20) for 5 min, incubated with secondary antibodies at RT and washed three times with TBST before being mounted with Prolong Diamond Anti-fade Mountant with DAPI (4',6-diamidino-2-phenylindole; Invitrogen). Photomicrographs of immunofluorescence staining were taken using a Leica DMRA fluorescence microscope with a Leica DFC360 FX camera (Leica, Wetzlar, Germany). Figures were assembled using Adobe Illustrator. The data are representative of at least three lungs from independent experiments.

### FACS analysis and cell sorting

Lungs from E18.5 embryonic mice were dissected and processed for flow cytometry analysis using BD LSR FORTRESSA™ (BD Bioscience). Isolation of epithelium and mesenchyme as well as isolation of AT2 cells was performed using the FACSARIA™ III (BD Bioscience) cell sorter. Following antibodies were used for analysis of AT1 and AT2 cell number [102513, 488-CD31 (1:50), Biolegend; 103108, FITC-CD45 (1:50); 118217, Apc Cy7 EpCam (1:50), or 47-5791-80, Apc-eFluor-780-EpCam (1:50), eBioscience; AB3786, proSPC (1:500), Millipore; 127409, Apc-Podoplanin (1:20), Biolegend; 402012, Apc Isotype Ctrl (1:20), Biolegend]. Fc block (Gamunex10%—1:10) was used for the blocking the non-specific binding and Saponin (558255, Cabiochem) was used for the permeabilization step. For the fluorescence-activated cell sorting of epithelium and mesenchyme, the cells were subsequently labeled with following antibodies [488-CD31 (1:50); FITC-CD45 (1:50); Apc

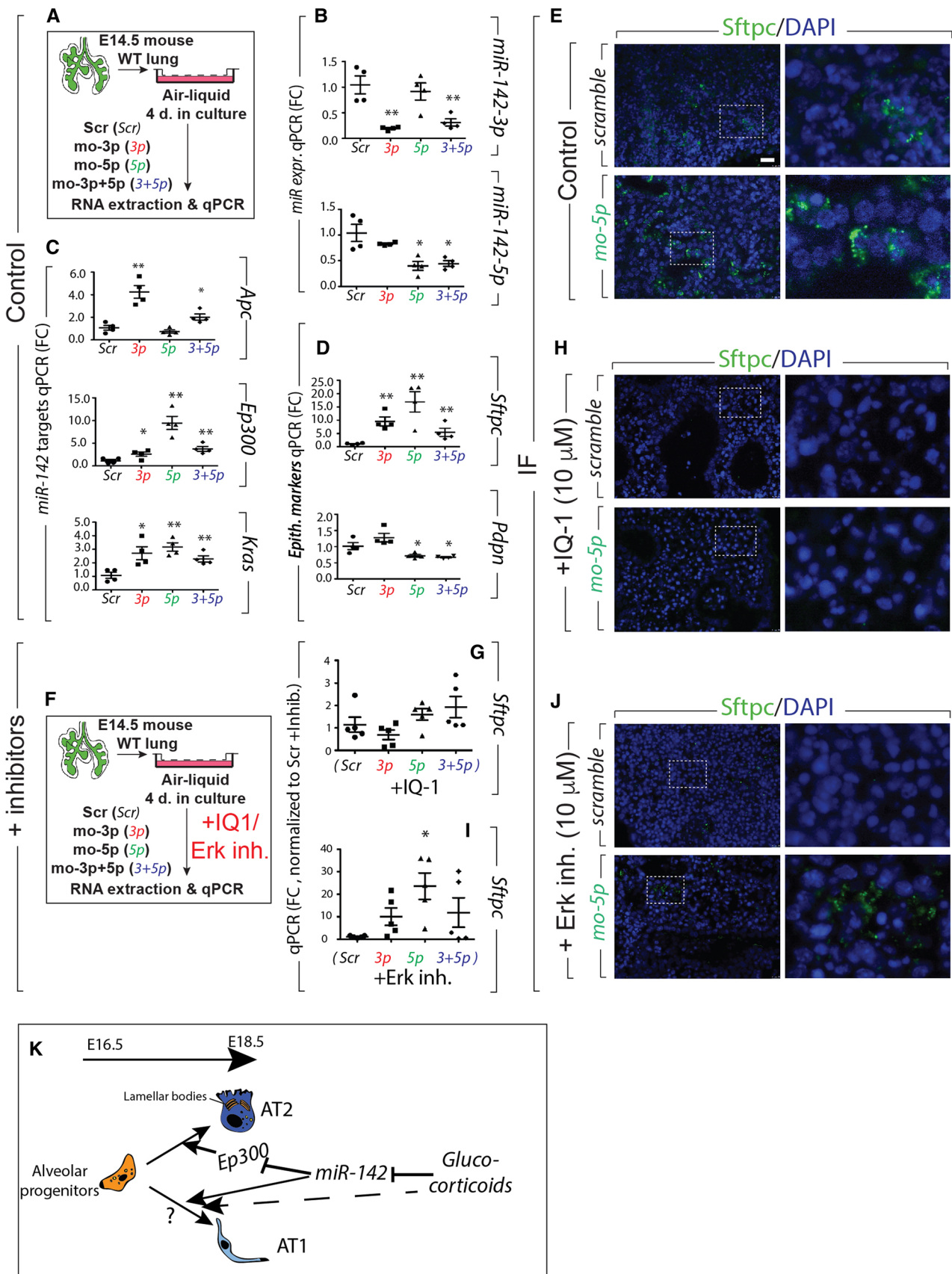


**Fig. 6** In vitro differentiation of the alveolar epithelial progenitors. **a** Schematic showing the in vitro treatment of E14.5 WT lung explants with morpholinos specific to *miR-142-3p* and *miR-142-5p* for 4 successive days ( $n=4$  for each condition). Impact of morpholino (*mo-3p*, *mo-5p*, *mo-(3p+5p)*) treatment on **b** *miR-142-3p* and *-5p* expression. **c** *Apc*, *Ep300* and *Kras* expression **d** *Sftpc*, *Pdpn* expression, **e** IF staining of *Sftpc* on E14.5 lung explants cultures treated with *Scramble* or *mo-5p* for 4 days. **f** Schematic showing the in vitro culture of E14.5 WT lung explants with *Scramble* or morpholinos against *miR-142-3p* or *-5p* for 4 successive days in presence of either IQ-1 (10  $\mu$ M) or SCH772984 (10  $\mu$ M) (a specific inhibitor of ERK1/2). qPCR analysis (**g–i**,  $n=5$ ) and IF staining (**h–j**) showing the level of expression of *Sftpc* on E14.5 lung explants cultures in presence of either IQ-1 or SCH772984 treated with morpholino specific to *miR-142-5p*. **k** Glucocorticoids (GC) are enhancing AT1 and AT2 formation. Inhibition of *miR-142* is sufficient to increase the AT2 to AT1 cell number ratio but does not perturb the flattening of the AT1 cells. It is still unclear whether *miR-142* acts directly or indirectly on the differentiation of the alveolar progenitors towards the AT1 lineage. Blockade of Ep300/ $\beta$ -catenin with IQ1 suppresses the increase in *Sftpc* expression triggered by the loss of *miR-142*. We propose that *miR-142* is a negative regulator of alveolar progenitor differentiation towards AT2 cells. In addition, GC can act in a *miR-142*-independent fashion to increase the differentiation of alveolar progenitors towards AT1 cells. Scale bar **e**, **h**, **j**: low mag: 16  $\mu$ m, high mag: 4  $\mu$ m

Cy7 EpCam (1:50)] whereas [488-CD31 (1:50); FITC-CD45 (1:50); Apc Cy7 EpCam (1:50), Apc-Podoplanin (Pdpn) (1:20); Apc Isotype Ctrl (1:20)] antibodies were used for isolation of AT1 and AT2 cells. Alveolar epithelial cells were identified as CD45<sup>-ve</sup>/CD31<sup>-ve</sup>/CD49f<sup>low</sup>/Epcam<sup>int</sup> and AT2 cells were identified as CD45<sup>-ve</sup>/CD31<sup>-ve</sup>/CD49f<sup>low</sup>/Epcam<sup>int</sup> and Pdpn<sup>-ve</sup> while AT1 cells were identified as CD45<sup>-ve</sup>/CD31<sup>-ve</sup>/CD49f<sup>low</sup>/Epcam<sup>int</sup> and Pdpn<sup>+ve</sup>. Cells were sorted through a flow chamber with a 100- $\mu$ m nozzle tip under 25 psi sheath fluid pressure. Isolated cells were used for RNA isolation. As a main criterion for gating, we used the settings allowing capturing 98% of the cells in the isotype control and then we applied these gating conditions to the stained cells.

### Microarray experiment

RNA was isolated using the RNeasy Mini Kit (217004; Qiagen). Purified total RNA was amplified using the Ovation PicoSL WTA System V2 kit (NuGEN). Per sample, 2  $\mu$ g amplified cDNA was Cy5-labeled using the SureTag DNA labeling kit (Agilent). 2  $\mu$ g of the labeled cDNA was hybridized on Agilent-074809 SurePrint G3 Mouse GE v2 8  $\times$  60 K Microarrays for 22 h at 65  $^{\circ}$ C in Agilent hybridization chambers. The cDNA was not fragmented before hybridization. Dried slides were scanned at 2  $\mu$ m/pixel resolution using the InnoScan 900 (Innopsys). The analysis was performed with R and the limma package. Gene set analyses were done using the Wilcoxon tests of the  $t$  statistics. The data are deposited in GEO and are available through the accession number GSE106411.

### Embryonic lung explant cultures

Timed pregnant wild-type mice were killed on E14.5, the embryonic lungs were harvested and placed on 8  $\mu$ m Nucleopore Track-Etch membranes (110414; Whatman). Vivo-morpholinos specific for *miR-142-3p* and/or *miR-142-5p* (Gene Tools LLC) were added at 5  $\mu$ M to E14.5 lung explants. Lungs were grown for 96 h at 37  $^{\circ}$ C with 5% CO<sub>2</sub> prior to analysis. In a second set of experiments, 100 nM dexamethasone (Dex, D1756; Sigma Aldrich), 10  $\mu$ M IQ-1 (Ep300/ $\beta$ -catenin (Ctnnb1) inhibitor, S8248; Selleckchem), 10  $\mu$ M SCH772984 (Erk inhibitor, 19166; CayMan Chemical) either alone or in combination with morpholinos were added to the E14.5 lung explants.

### Western blotting

Immunoblotting was performed using antibodies against pro-Sftpc (AB3786, Millipore; 1:1000), Lamin B1 (B-10) (sc-374015 from SantaCruz; 1:200) and beta-actin (ab8227, Abcam; 1:50000).

### Statistical analysis

Data were assembled using Graph Pad Prism Software (Graph Pad software, USA) and presented as average values  $\pm$  S.E.M. Statistical analyses were performed using Student's  $t$  test. Data were considered significant if  $p < 0.05$ . Figures were assembled using Adobe Photoshop CS6 and Adobe Illustrator CS6.

**Acknowledgements** We acknowledge the precious help provided by Kerstin Goth and Jana Rostkovius in managing the mouse colonies, and Shirisha Bagari for the genotyping of the mice. C.M.C. and E.E.A. were funded by start-up grants from the Cardio Pulmonary Institute (CPI) (previously known as Excellence Cluster Cardio-Pulmonary System (ECCPS)). C.M.C. also acknowledges the support of the University Hospital Giessen and Marburg (UKGM). E.E.A. acknowledges the support of the University Hospital Giessen and Marburg (UKGM) and the German Center for Lung Research (DZL). S.B. was supported by grants from the Deutsche Forschungsgemeinschaft (DFG; BE4443/1-1, BE4443/4-1, BE4443/6-1, BE4443/14-1, KFO309 P7 and SFB1213-projects A02 and A04), UKGM, Universities of Giessen and Marburg Lung Center (UGMLC) and the Deutsche Zentrum für Lungenforschung (DZL). J.S.Z was funded through a start-up package from Wenzhou Medical University and the National Natural Science Foundation of China (Grant Number 81472601). S.H. was supported by University Hospital Giessen and Marburg (FOKOOPV), the German Center for Lung Research (DZL), and Grants from the DFG (KFO309 P2/8; SFB1021 C05, SFB TR84 B2). CC was supported by the Interventional Pulmonary Key Laboratory of Zhejiang Province, the Interventional Pulmonology Key Laboratory of Wenzhou City, the Interventional Pulmonology Innovation Subject of Zhejiang Province, the National Nature Science Foundation of China (81570075, 81770074), Zhejiang Provincial Natural Science Foundation (LZ15H010001), Zhejiang Provincial Science Technology

Department Foundation (2015103253) as well as the National Key Research and Development Program of China (2016YFC1304000). B.M. acknowledges the ANR-18-CE92-0009-01.

## References

- McCulley D, Wienhold M, Sun X (2015) The pulmonary mesenchyme directs lung development. *Curr Opin Genet Dev* 32:98–105
- El Agha E, Bellusci S (2014) Walking along the fibroblast growth factor 10 route: a key pathway to understand the control and regulation of epithelial and mesenchymal cell-lineage formation during lung development and repair after injury. *Scientifica* 2014:538379
- Rawlins EL, Clark CP, Xue Y, Hogan BL (2009) The Id2+ distal tip lung epithelium contains individual multipotent embryonic progenitor cells. *Development* 136:3741–3745
- Rockich BE, Hrycaj SM, Shih HP, Nagy MS, Ferguson MA, Kopp JL, Sander M, Wellik DM, Spence JR (2013) Sox9 plays multiple roles in the lung epithelium during branching morphogenesis. *Proc Natl Acad Sci USA* 110:E4456–E4464
- Treutlein B, Brownfield DG, Wu AR, Neff NF, Mantalas GL, Espinoza FH, Desai TJ, Krasnow MA, Quake SR (2014) Reconstructing lineage hierarchies of the distal lung epithelium using single-cell RNA-seq. *Nature* 509:371–375
- Li J, Wang Z, Chu Q, Jiang K, Li J, Tang N (2018) The strength of mechanical forces determines the differentiation of alveolar epithelial cells. *Dev Cell* 44:297–312 e295
- Jonas S, Izaurralde E (2015) Towards a molecular understanding of microRNA-mediated gene silencing. *Nat Rev Genet* 16:421–433
- Shrestha A, Mukhametshina RT, Taghizadeh S, Vasquez-Pacheco E, Cabrera-Fuentes H, Rizvanov A, Mari B, Carraro G, Bellusci S (2017) MicroRNA-142 is a multifaceted regulator in organogenesis, homeostasis, and disease. *Dev Dyn* 246:285–290
- Carraro G, Shrestha A, Rostkovich J, Contreras A, Chao CM, El Agha E, Mackenzie B, Dilai S, Guidolin D, Taketo MM, Gunther A, Kumar ME, Seeger W, De Langhe S, Barreto G, Bellusci S (2014) miR-142-3p balances proliferation and differentiation of mesenchymal cells during lung development. *Development* 141:1272–1281
- Sun Y, Kolligs FT, Hottiger MO, Mosavin R, Fearon ER, Nabel GJ (2000) Regulation of beta-catenin transformation by the p300 transcriptional coactivator. *Proc Natl Acad Sci USA* 97:12613–12618
- Sharma S, Liu J, Wei J, Yuan H, Zhang T, Bishopric NH (2012) Repression of miR-142 by p300 and MAPK is required for survival signalling via gp130 during adaptive hypertrophy. *EMBO Mol Med* 4:617–632
- Shrestha A, Carraro G, El Agha E, Mukhametshina R, Chao CM, Rizvanov A, Barreto G, Bellusci S (2015) Generation and validation of miR-142 knock out mice. *PLoS One* 10:e0136913
- Laresgoiti U, Nikolic MZ, Rao C, Brady JL, Richardson RV, Batchen EJ, Chapman KE, Rawlins EL (2016) Lung epithelial tip progenitors integrate glucocorticoid- and STAT3-mediated signals to control progeny fate. *Development* 143:3686–3699
- Kotton DN, Morrisey EE (2014) Lung regeneration: mechanisms, applications and emerging stem cell populations. *Nat Med* 20:822–832
- Desai TJ, Brownfield DG, Krasnow MA (2014) Alveolar progenitor and stem cells in lung development, renewal and cancer. *Nature* 507:190–194
- Chao CM, Yahya F, Moiseenko A, Tiozzo C, Shrestha A, Ahmadvand N, El Agha E, Quantius J, Dilai S, Kheirollahi V, Jones M, Wilhem J, Carraro G, Ehrhardt H, Zimmer KP, Barreto G, Ahlbrecht K, Morty RE, Herold S, Abellar RG, Seeger W, Schermuly R, Zhang JS, Minoo P, Bellusci S (2017) Fgf10 deficiency is causative for lethality in a mouse model of bronchopulmonary dysplasia. *J Pathol* 241:91–103
- Ramasamy SK, Mailloux AA, Gupte VV, Mata F, Sala FG, Veltmaat JM, Del Moral PM, De Langhe S, Parsa S, Kelly LK, Kelly R, Shia W, Keshet E, Minoo P, Warburton D, Bellusci S (2007) Fgf10 dosage is critical for the amplification of epithelial cell progenitors and for the formation of multiple mesenchymal lineages during lung development. *Dev Biol* 307:237–247
- Herriges JC, Verheyden JM, Zhang Z, Sui P, Zhang Y, Anderson MJ, Swing DA, Zhang Y, Lewandoski M, Sun X (2015) FGF-regulated ETV transcription factors control FGF-SHH feedback loop in lung branching. *Dev Cell* 35:322–332
- Mailloux AA, Tefft D, Ndiaye D, Itoh N, Thiery JP, Warburton D, Bellusci S (2001) Evidence that SPROUTY2 functions as an inhibitor of mouse embryonic lung growth and morphogenesis. *Mech Dev* 102:81–94
- McQualter JL, Yuen K, Williams B, Bertonecello I (2010) Evidence of an epithelial stem/progenitor cell hierarchy in the adult mouse lung. *Proc Natl Acad Sci USA* 107:1414–1419
- Weiss DJ, Kolls JK, Ortiz LA, Panoskaltis-Mortari A, Prockop DJ (2008) Stem cells and cell therapies in lung biology and lung diseases. *Proc Am Thorac Soc* 5:637–667
- Zemke AC, Teisanu RM, Giangreco A, Drake JA, Brockway BL, Reynolds SD, Stripp BR (2009) beta-Catenin is not necessary for maintenance or repair of the bronchiolar epithelium. *Am J Respir Cell Mol Biol* 41:535–543
- Wang Y, Frank DB, Morley MP, Zhou S, Wang X, Lu MM, Lazar MA, Morrisey EE (2016) HDAC3-dependent epigenetic pathway controls lung alveolar epithelial cell remodeling and spreading via miR-17-92 and TGF-beta signaling regulation. *Dev Cell* 36:303–315
- Carraro G, El-Hashash A, Guidolin D, Tiozzo C, Turcatel G, Young BM, De Langhe SP, Bellusci S, Shi W, Parnigotto PP, Warburton D (2009) miR-17 family of microRNAs controls FGF10-mediated embryonic lung epithelial branching morphogenesis through MAPK14 and STAT3 regulation of E-Cadherin distribution. *Dev Biol* 333:238–250
- Wang X, Wang Y, Snitow ME, Stewart KM, Li S, Lu M, Morrisey EE (2016) Expression of histone deacetylase 3 instructs alveolar type I cell differentiation by regulating a Wnt signaling niche in the lung. *Dev Biol* 414:161–169
- Alanis DM, Chang DR, Akiyama H, Krasnow MA, Chen J (2014) Two nested developmental waves demarcate a compartment boundary in the mouse lung. *Nat Commun* 5:3923
- Rieger ME, Zhou B, Solomon N, Sunohara M, Li C, Nguyen C, Liu Y, Pan JH, Minoo P, Crandall ED, Brody SL, Kahn M, Borok Z (2016) p300/beta-catenin interactions regulate adult progenitor cell differentiation downstream of WNT5a/protein kinase C (PKC). *J Biol Chem* 291:6569–6582
- Sasaki T, Kahn M (2014) Inhibition of beta-catenin/p300 interaction proximalizes mouse embryonic lung epithelium. *Transl Respir Med* 2:8
- Sladitschek HL, Neveu PA (2015) The bimodally expressed microRNA miR-142 gates exit from pluripotency. *Mol Syst Biol* 11:850
- Chang DR, Martinez Alanis D, Miller RK, Ji H, Akiyama H, McCrea PD, Chen J (2013) Lung epithelial branching program antagonizes alveolar differentiation. *Proc Natl Acad Sci USA* 110:18042–18051

**Publisher's Note** Springer Nature remains neutral with regard to jurisdictional claims in published maps and institutional affiliations.